

RAG Mutations in Human B Cell-Negative SCID

Klaus Schwarz,* George H. Gauss, Leopold Ludwig, Ulrich Pannicke, Zhong Li, Doris Lindner, Wilhelm Friedrich, Reinhard A. Seger, Thomas E. Hansen-Hagge, Stephen Desiderio, Michael R. Lieber, Claus R. Bartram†

Patients with human severe combined immunodeficiency (SCID) can be divided into those with B lymphocytes (B⁺ SCID) and those without (B⁻ SCID). Although several genetic causes are known for B⁺ SCID, the etiology of B⁻ SCID has not been defined. Six of 14 B⁻ SCID patients tested were found to carry a mutation of the recombinase activating gene 1 (*RAG-1*), *RAG-2*, or both. This mutation resulted in a functional inability to form antigen receptors through genetic recombination and links a defect in one of the site-specific recombination systems to a human disease.

Site-directed recombination in the human immune system is essential for the generation of antigen-binding diversity by assembly of the variable (V), diversity (D), and joining (J) domain exons at the immunoglobulin and T cell receptor gene loci during lymphocyte development. Two lymphoid-specific genes, *RAG-1* and *RAG-2*, together confer V(D)J recombination activity on artificial substrates in lymphocytes or nonlymphoid cells (1, 2). Gene-targeted mice with a deletion of the *RAG-1* or *RAG-2* gene lack mature B and T cells because of an inability to initiate V(D)J recombination (3). The *RAG-1* and *RAG-2* proteins have endonuclease activity at V(D)J recombination signal sequences (4).

Human SCID comprises a group of genotypically and phenotypically heterogeneous diseases (5). SCID immunophenotypes can be classified according to the presence (B⁺ SCID) or absence (B⁻ SCID) of B cells in the peripheral blood of the patient. There are several causes of the more common B⁺ SCID phenotype (70%

of all SCID cases), including defects in the γ chain common to the receptors for interleukin-2, -4, -7, -9, and -15 (ILR γ_c) (6); defects in adenosine deaminase (7) or purine nucleoside phosphorylase (8); inappropriate regulation of human leukocyte antigen (HLA) class II expression (9); defective IL-2 production (10); and impairments in the T cell receptor-CD3 complex (11) or T cell signal transduction pathways (12). The most seriously affected SCID patients are those without detectable B cells (30% of all SCID patients). In contrast to other SCID subgroups, B⁻ SCID is associated with irregular V(D)J recombination events at the antigen receptor loci (13).

The DNA samples of 35 healthy blood donor controls and 30 SCID patients (14 B⁻ SCID and 16 B⁺ SCID patients) were analyzed. Mutations were detected through the use of single-strand conformation polymorphism (SSCP) assays with primer cassettes overlapping the entire *RAG-1* and *RAG-2* coding regions. Four B⁻ SCID patients in four families exhibited an altered migration pattern for *RAG-1* amplimers. Three B⁻ SCID patients in two families exhibited an altered migration pattern for *RAG-2* amplification products. To verify the SSCP findings and to identify the nature of the possible mutations, we sequenced polymerase chain reaction (PCR) products directly three times for each candidate mutation. Five missense, three nonsense, and one deletion mutation were detected (Table 1). All of the mutations were inherited. Consanguinity contributes to the occurrence of inherited SCID because the parents of P2 [homozygous for a *RAG-1* T(2926)→G transversion] have common great-great-grandparents. The patients P5 and P6 are siblings of first-degree cousins within a highly inbred family; both are homozygous for a G(2634)→A transition of *RAG-2* (Table 1). None of the mutations was detected in B⁺ SCID patients or in 35

healthy subjects. Several of the SCID patients had unaffected siblings who were heterozygous with a single wild-type allele for *RAG-1* or *RAG-2* (Table 1). Thus, the presence of one wild-type allele seems to be sufficient for normal lymphocyte development. Deletion mutagenesis has defined a core fragment of murine *RAG-1* (amino acids 384 to 1009) (14). All human *RAG-1* substitutional mutations are located within this core at conserved residues. Residues 383 to 527 of murine *RAG-2* are dispensable for V(D)J recombination (15). The human *RAG-2* mutation Cys⁴⁷⁸→Tyr lies within that region. This paradoxical result is consistent with the previously published observation that a substitution at position 436 of murine *RAG-2* resulted in a 5% residual activity, whereas the deletion of residues 383 to 527 resulted in only a 50% reduction (15).

To determine whether the SCID-associated *RAG-1* and *RAG-2* mutations are associated with impaired V(D)J recombination activity, we performed transient transfection assays (16) in the human fibroblast cell line 293 using expression vectors encoding each of the mutant *RAG-1* and *RAG-2* proteins. Wild-type human *RAG-1* and *RAG-2* yielded V(D)J recombination frequencies of $\sim 0.1 \pm 0.08\%$ (mean \pm SD)

Table 1. *RAG-1* and *RAG-2* mutations in B⁻ SCID patients. Genomic patient DNA was obtained from polymorphic nuclear cells (PNCs) of the peripheral blood (P1 and P2), mononuclear cells of the blood (P3) and bone marrow (P6), and primary fibroblast lines (P4 and P5). DNA of the patients' relatives and controls was obtained from PNCs.

Patient (sex)	Allele*	Mutation†	Amino acid change
<i>RAG-1</i>			
P1 (m)‡	m	G(2276)→A	Glu ⁷²² →Lys
	p	G(2432)→T	Glu ⁷⁷⁴ →Stop
P2 (f)	m	T(2926)→G	Tyr ⁹³⁸ →Stop
	p	T(2926)→G	Tyr ⁹³⁸ →Stop
P3 (m)¶	m	C(579)→T	Ala ¹⁵⁶ →Val
	p	Del	-
P4 (m)#	m	C(2801)→T	Arg ⁸⁹⁷ →Stop
	p	G(1983)→A	Arg ⁶²⁴ →His
<i>RAG-2</i>			
P5 (f)** and P6 (m)	m	G(2634)→A	Cys ⁴⁷⁸ →Tyr
	p	G(2634)→A	Cys ⁴⁷⁸ →Tyr
P3 (m)¶	m	G(1887)→A	Arg ²²⁹ →Gln
	p	Del	-

*Maternal (m) or paternal (p) alleles are indicated. †Nucleotide numbering according to Schatz *et al.* (1) for *RAG-1* and according to Ichihara *et al.* (21) for *RAG-2*. ‡One sister heterozygous for Glu⁷²²→Lys. ||One brother and sister heterozygous for Tyr⁹³⁸→Stop. ¶Deceased sibling not tested; the paternal deletion encompassed the total *RAG-1* and *RAG-2* locus on chromosome 11p13; the break points were not determined. #One sister homozygous for wild type. **One other brother heterozygous for Cys⁴⁷⁸→Tyr.

K. Schwarz and C. R. Bartram, Section of Molecular Biology and Department of Pediatrics II, University of Ulm, D-89070 Ulm, Germany.

G. H. Gauss and M. R. Lieber, Department of Pathology, School of Medicine, Washington University, St. Louis, MO 63110, USA.

L. Ludwig, Department of Internal Medicine I, University of Ulm, D-89070 Ulm, Germany.

U. Pannicke, D. Lindner, T. E. Hansen-Hagge, Section of Molecular Biology, University of Ulm, D-89070 Ulm, Germany.

Z. Li and S. Desiderio, Department of Molecular Biology and Genetics and Howard Hughes Medical Institute, School of Medicine, Johns Hopkins University, Baltimore, MD 21205, USA.

W. Friedrich, Department of Pediatrics II, University of Ulm, D-89070 Ulm, Germany.

R. A. Seger, University Children's Hospital, University of Zürich, Zürich, Switzerland.

*To whom correspondence should be addressed at the Department of Transfusion Medicine, University of Ulm, Helmholzstraße 10, D-89081 Germany. E-mail: klaus.schwarz@medizin.uni-ulm.de

†Present address: Institute of Human Genetics, University of Heidelberg, D-69120 Heidelberg, Germany.

for signal joints and $0.09 \pm 0.1\%$ for coding joints (Table 2). One of the RAG-1 mutants (RAG-1 Ala¹⁵⁶→Val) gave recombination efficiencies similar to those of wild type, indicating that this mutation is a functional polymorphism. For the other mutants, recombination values were typically 0.1 to 1% of wild type for both coding and signal joint formation (Table 2).

The rare signal and coding joints that were detected from the mutant RAG-1 and RAG-2 transfections were sequenced to determine whether there was any qualitative difference between them and junctions generated with wild-type RAG-1 and RAG-2. In wild-type human cells, most signal joints are precise, with 3% or less showing nucleotide loss. Rare signal joints formed from the mutant RAGs were all precise. Like-

wise, sequences of rare coding joints formed by the mutant RAGs were qualitatively indistinguishable from normal (17). In wild-type human cells, there exists a range of nucleotide loss and addition in coding joints (18). We find similar features in the rare coding joints generated by the mutant RAGs. Thus, although the mutant RAGs result in a marked decrease in recombination efficiency, the few signal and coding joints that do occur are qualitatively indistinguishable from wild type, indicating that the enzymatic steps that occur after the initial DNA breaks induced by the RAG proteins are unaffected by these mutations. The immunophenotype of the patients was consistent with the loss of V(D)J recombination activity (19).

The RAG mutations associated with B⁻

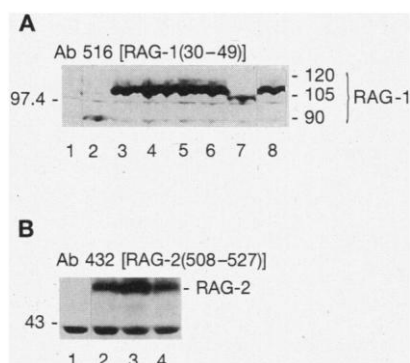
SCID do not affect steady-state RAG protein levels, nor do they affect subcellular localization of RAG-1 and RAG-2. Immunoblots for RAG-1 (Fig. 1A) and RAG-2 (Fig. 1B) with extracts from transfected 293 cells indicate expression within a factor of 3 after transfection with wild-type and mutant RAG-1 and RAG-2. Subcellular localization of human RAGs was not affected by the SCID-associated mutations. Wild-type as well as mutant RAG-1 and RAG-2 proteins were predominantly evenly distributed within the nucleus, with the nucleoli less intensely stained (17).

In summary, we describe human autosomal recessive SCID patients with nonsense, missense, and deletional mutations in the RAG-1 or RAG-2 genes, or both. This result links a defect in one of the site-directed recombination systems to a human disease. The RAG-1 and RAG-2 alterations exhibit either a complete loss or a marked reduction of V(D)J recombination activity. Impairment of V(D)J recombination is accompanied by the absence of B cells in all patients. Patient T cells are absent in most cases but present in one patient because of a leaky mutation (19). Approximately half of B⁻ SCID patients tested carried RAG mutations. Given that B⁻ SCID cases constitute about 30% of all human SCID patients, these data suggest that structural mutations in RAG genes may account for a substantial proportion of human SCID cases.

Table 2. Recombination frequency of RAG-1 and RAG-2 mutants. Recombination frequencies were determined in human 293 fibroblasts by the extrachromosomal V(D)J assay (16, 18). Recombination frequencies represent the mean of four or more independent experiments; background V(D)J recombination frequency: $<1 \times 10^{-8}$. WT, wild type; DpnI^r, resistant to DpnI digest.

Expression vectors	Signal or coding junctions	$\cdot 10^6$ total DpnI ^r colonies screened	Recombination frequency (%)	Fold reduction of mutants relative to wild type
R1WT/R2WT	SJ	1.5	0.10	-
	CJ	1.8	0.09	-
R1(Glu ⁷²² →Lys)/R2WT	SJ	1.6	0.0003	326
	CJ	1.7	<0.0005	>196
R1(Tyr ⁹³⁸ →Stop)/R2WT	SJ	2.3	0.0006	157
	CJ	5.8	<0.00006	>1378
R1(Ala ¹⁵⁶ →Val)/R2WT	SJ	0.8	0.07	1.5
	CJ	1.4	0.12	0.7
R1(Arg ⁶²⁴ →His)/R2WT	SJ	0.6	<0.0007	>140
	CJ	2.3	0.0002	577
R1WT/R2(Cys ⁴⁷⁸ →Tyr)	SJ	0.6	0.001	84
	CJ	1.8	0.0001	736
R1WT/R2(Arg ²²⁹ →Gln)	SJ	1.9	0.0006	170
	CJ	2.6	<0.0002	>510
R1(Ala ¹⁵⁶ →Val)/R2(Arg ²²⁹ →Gln)	SJ	12.5	0.001	81
	CJ	6.3	0.0008	114

Fig. 1. Protein analysis of RAG-1 and RAG-2 mutants (22). **(A)** Steady-state levels of mutant and wild-type RAG-1 proteins in transfected 293 human fibroblasts. Protein from transfected 293 cells was detected by immunoblotting with antibody 516 specific for RAG-1. Lane 1, empty vector; lane 2, RAG-1(Glu⁷⁷⁴→Stop); lane 3, RAG-1(Glu⁷²²→Lys); lane 4, RAG-1(Tyr⁹³⁸→Stop); lane 5, RAG-1(Ala¹⁵⁶→Val); lane 6, RAG-1(Arg⁶²⁴→His); lane 7, RAG-1(Arg⁶⁹⁷→Stop); lane 8, wild-type human RAG-1. RAG protein expression for the various mutants was within a factor of 3 of each other. Immunoblotting with antibody 306 supported this result (17); only RAG-1 proteins without premature stop codons were stained. **(B)** Steady-state levels of mutant and wild-type RAG-2 proteins. Protein from transfected cells was detected by immunoblotting with antibody 432 specific for RAG-2. Lane 1, empty vector; lane 2, wild-type human RAG-2; lane 3, RAG-2(Cys⁴⁷⁸→Tyr); lane 4, RAG-2(Arg²²⁹→Gln). Immunoblotting with antibody 435 gave similar results. The position of murine and human RAG proteins is indicated at right. Antibodies 516 and 306 are directed against phylogenetically conserved residues 30 to 49 and 959 to 977, respectively, of mouse RAG-1; antibodies 432 and 435 are directed against residues 508 to 527 and 339 to 411, respectively, of mouse RAG-2 (20).



REFERENCES AND NOTES

- D. G. Schatz, M. A. Oettinger, D. Baltimore, *Cell* **59**, 1035 (1989).
- M. A. Oettinger, D. G. Schatz, C. Gorka, D. Baltimore, *Science* **248**, 1517 (1990).
- P. Mombaerts *et al.*, *Cell* **68**, 869 (1992); Y. Shinkai *et al.*, *ibid.*, p. 855.
- J. F. McBlane *et al.*, *ibid.* **83**, 387 (1995).
- A. Fischer, *Immunodef. Rev.* **3**, 83 (1992).
- M. Noguchi *et al.*, *Cell* **73**, 147 (1993); D. J. Matthews *et al.*, *Blood* **85**, 38 (1995).
- R. Hirschhorn, *Pediatr. Res.* **33** (suppl. 1), 35 (1993).
- M. L. Markert, *Immunodef. Rev.* **3**, 45 (1991).
- V. Steimle, L. A. Otten, M. Zufferey, B. Mach, *Cell* **75**, 135 (1993); V. Steimle *et al.*, *Genes Dev.* **9**, 1021 (1995).
- K. Weinberg and R. Parkman, *N. Engl. J. Med.* **322**, 1718 (1990).
- V. A. Armaiz *et al.*, *ibid.* **327**, 529 (1992); C. Soudais, J. de Villartay, F. Le Deist, A. Fischer, G. B. Lisowska, *Nature Genet.* **3**, 77 (1993).
- T. Chatila *et al.*, *Proc. Natl. Acad. Sci. U.S.A.* **87**, 10033 (1990); E. Arpaia, M. Shahar, H. Dadi, A. Cohen, C. M. Roifman, *Cell* **76**, 947 (1993); A. C. Chan *et al.*, *Science* **264**, 1599 (1994); M. E. Elder *et al.*, *ibid.*, p. 1596; P. Macchi *et al.*, *Nature* **376**, 65 (1995); S. M. Russell *et al.*, *Science* **270**, 797 (1995).
- K. Schwarz *et al.*, *J. Exp. Med.* **174**, 1039 (1991); T. Abe *et al.*, *J. Immunol.* **152**, 5504 (1994).
- M. J. Sadofsky *et al.*, *Nucleic Acids Res.* **21**, 5644 (1993); D. P. Silver, E. Spanopoulou, R. C. Mulligan, D. Baltimore, *Proc. Natl. Acad. Sci. U.S.A.* **90**, 6100 (1993).
- M. J. Sadofsky *et al.*, *Nucleic Acids Res.* **22**, 1805 (1994); C. A. Cuomo and M. A. Oettinger, *ibid.*, p. 1810.
- G. H. Gauss and M. R. Lieber, *Mol. Cell. Biol.* **13**, 3900 (1993).

17. K. Schwarz, G. H. Gauss, Z. Li, S. Desiderio, M. R. Lieber, unpublished results.
18. G. H. Gauss and M. R. Lieber, *Mol. Cell. Biol.* **16**, 258 (1996).
19. Immunophenotypes of patients with RAG mutations were obtained from routine clinical specimens at the admission of the patients. B cells (CD20) and T cells (CD3) are expressed as a percentage of total peripheral blood mononuclear cells (PBMCs): P1: 0% CD20, 0% CD3; P2: 0% CD20, 15% CD3; P3: 0% CD20, 59% CD3; P4: 0% CD20, 15% CD3; P5: 0% CD20, 0% CD3; and P6: 1% CD20, 70% CD3. The CD3-positive cells in P2, P4, and P6 were identified as maternal T cells by HLA typing. The CD3-positive cells in P3 were of patient origin as assessed by HLA classification and minisatellite analysis. The CD3 cells were not revertants because no wild-type RAG signal was detected in PCR or SSCP in MNCs of the patient. V_{α} and V_{β} repertoires were addressed by reverse transcriptase-PCR in PBMCs and exhibited an oligoclonal pattern. Thus, patient P3 was considered leaky.
20. W.-C. Lin and S. Desiderio, *Science* **260**, 953 (1993).
21. Y. Ichikara, M. Hirai, Y. Kurosawa, *Immunol. Lett.* **33**, 272 (1992).
22. RAG-1 and RAG-2 expression vectors used for all recombination assays were identical except for the single mutation introduced; thus, promoter and 5' and 3' untranslated region influences on expression are excluded. Cells transfected with RAG expression vectors were boiled in SDS lysis buffer. Equal amounts of total protein (100 μ g) were fractionated by 10% SDS-polyacrylamide gel electrophoresis. Protein was transferred to nitrocellulose and detected by immunoblotting with affinity-purified antibodies to RAG as described (20).
23. K.S., U.P., D.L., and C.R.B. are recipients of grants of the Sonderforschungsbereich 322 from the Deutsche Forschungsgemeinschaft. G.H.G. is supported by a PHS grant awarded to the Stanford University Program in Cancer Biology. M.R.L. is a Leukemia Society of America Scholar, and research in his laboratory is supported by grants from the NIH and a grant from the Council for Tobacco Research. S.D. is supported by a grant from the National Cancer Institute and by the Howard Hughes Medical Institute.

3 June 1996; accepted 20 August 1996

Correlative Memory Deficits, A β Elevation, and Amyloid Plaques in Transgenic Mice

Karen Hsiao,* Paul Chapman, Steven Nilsen, Chris Eckman, Yasuo Harigaya, Steven Younkin, Fusheng Yang, Greg Cole

Transgenic mice overexpressing the 695-amino acid isoform of human Alzheimer β -amyloid (A β) precursor protein containing a Lys⁶⁷⁰ \rightarrow Asn, Met⁶⁷¹ \rightarrow Leu mutation had normal learning and memory in spatial reference and alternation tasks at 3 months of age but showed impairment by 9 to 10 months of age. A fivefold increase in A β (1–40) and a 14-fold increase in A β (1–42/43) accompanied the appearance of these behavioral deficits. Numerous A β plaques that stained with Congo red dye were present in cortical and limbic structures of mice with elevated amounts of A β . The correlative appearance of behavioral, biochemical, and pathological abnormalities reminiscent of Alzheimer's disease in these transgenic mice suggests new opportunities for exploring the pathophysiology and neurobiology of this disease.

Alzheimer's disease (AD), the most common cause of dementia in aged humans, is a disease of unknown etiology. Amyloid plaques are routinely used for diagnosing AD in brain tissue (1), even though other histologic changes such as neurofibrillary tangles, synaptic and neuronal loss, and dystrophic neurites are also usually present and sometimes correlate better with dementia (2, 3). The amyloid in senile plaques is composed of A β , a 39- to 43-amino acid protein derived from the larger amyloid precursor protein (APP). Small numbers of

classic senile plaques develop in the brain with age, but large numbers of senile plaques are found almost exclusively in patients with Alzheimer's type dementia. A diagnosis of AD is made only if both cognitive deterioration and senile plaques are present (4). APP isoforms resulting from alternative splicing form a set of polypeptides ranging from 563 to 770 residues in length. The most abundant of these, APP₆₉₅, is predominantly expressed in neurons (5) and lacks a Kunitz-protease inhibitor (KPI) domain present in the APP₇₅₁ and APP₇₇₀ isoforms. Five mutations in APP, all located in or near the A β domain, have been identified in families with early-onset AD (6–10).

Transgenic mice (Swiss Webster \times C57B6/DBA2) expressing three isoforms of mutant APP (Val⁷¹⁷ \rightarrow Phe) with an overrepresentation of KPI-containing isoforms showed Alzheimer-type neuropathology, including abundant thioflavin S-positive A β deposits, neuritic plaques, synaptic loss, as-

trocytosis, and microgliosis (11), but deficits in memory and learning have not yet been reported. Transgenic mice (JU) expressing human wild-type APP₇₅₁ showed deficits in spatial reference and alternation tasks by 12 months of age (12). However, only 4% of aged (\geq 12 months) transgenic mice exhibited A β deposits, and these were rare and diffuse and did not stain with Congo red dye (13). Transgenic mice (FVB/N) overexpressing wild-type and variant human or mouse APP₆₉₅ developed a central nervous system disorder that involved most of the corticolimbic regions of the brain (except the somatosensorimotor area) and resembled an accelerated naturally occurring senescent disorder of FVB/N mice (14). Parameters that influence the phenotype of transgenic mice expressing APP include host strain, APP primary structure, and extent of APP expression (14). We investigated the effects of APP overexpression in C57B6/SJL F₂ mice backcrossed to C57B6 breeders because of their greater longevity compared with FVB/N mice expressing identical transgenes.

Human APP₆₉₅ containing the double mutation Lys⁶⁷⁰ \rightarrow Asn, Met⁶⁷¹ \rightarrow Leu (K670N,M671L; APP₇₇₀ numbering), which was found in a large Swedish family with early-onset AD (10), was inserted into a hamster prion protein (PrP) cosmid vector (15) in which the PrP open reading frame (ORF) was replaced with the variant APP ORF [see (14)]. The resulting mice, Tg(HuAPP695.K670N-M671L)2576, produced 5.56 ± 0.33 units (mean \pm SEM; 73-day-old mice) to 5.76 ± 0.74 units (430-day-old mice) of transgenic brain APP expression, where a unit of expression is equivalent to the amount of endogenous mouse APP in nontransgenic (control) littermates (Fig. 1). Transgenic APP expres-

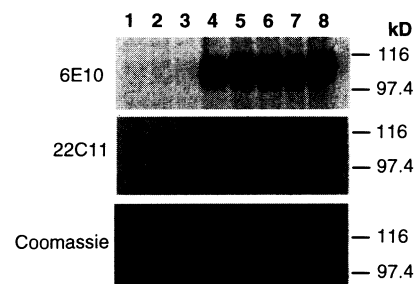


Fig. 1. Brain APP immunoblot of young and old Tg⁺ mice and nontransgenic control mice with 6E10 (24), which recognizes human but not mouse APP, and 22C11 (Boehringer Mannheim), which recognizes both human and mouse APP. Lanes 1 to 3, nontransgenic mice; lanes 4 to 6, 73-day-old mice; lanes 7 and 8, 430-day-old mice. Detailed methods for APP quantitation were described previously (14); antibody binding was revealed with ³⁵S-labeled protein A instead of ¹²⁵I-labeled protein A.

K. Hsiao and S. Nilsen, Department of Neurology, UMHC Box 295, 420 Delaware Street, University of Minnesota, Minneapolis, MN 55455, USA.

P. Chapman, Physiology Unit, University of Wales, Cardiff CF1 3US, UK.

C. Eckman, Y. Harigaya, S. Younkin, Mayo Clinic Jacksonville, Jacksonville, FL 32224, USA.

F. Yang and G. Cole, GRECC, Veterans Administration Medical Center, Sepulveda, CA 91343, USA, and Departments of Medicine and Neurology, University of California, Los Angeles, CA 91343, USA.

*To whom correspondence should be addressed.